AIMS Materials Science, 6(5): 635–645.
DOI: 10.3934/matersci.2019.5.635
Received: 01 May 2019
Accepted: 14 July 2019
Published: 16 July 2019

http://www.aimspress.com/journal/Materials

Research article

Experimental investigation of cutting parameters dependence in diamond turning of monocrystalline silicon

Lu Liao[1], Guo Li[1,*] and Junjie Zhang[2,*]

[1] Laser Fusion Research Center, China Academy of Engineering Physics, Mianyang 621900, China
[2] Center for Precision Engineering, Harbin Institute of Technology, Harbin 150001, China

*** Correspondence:** Email: liguo51404@163.com; zhjj505@gmail.com.

Abstract: The machinability of brittle materials is strongly dependent on machining conditions. In the present work, we perform ultra-precision single point diamond turning experiments of monocrystalline Si(100) using diamond cutting tools. The machined surface quality is characterized by evaluating surface topography and surface integrity. Systematic investigation of cutting parameters dependence of machining results is performed by considering rake angle of cutting tool, depth of cut and spindle speed. Experimental results suggest an optimized combination of cutting parameters for the best surface quality of Si(100) by diamond turning.

Keywords: monocrystalline silicon; diamond turning; surface integrity; rake angle

1. Introduction

Silicon (Si) as an important semiconductor material has been widely used for electronic devices manufacturing, due to its excellent physical and mechanical properties. Achieving ultra-smooth surface is important for the performance of Si-based devices, thus various kinds of manufacturing techniques have been proposed. In particular, ultra-precision single point diamond turning (SPDT) has been demonstrated as an effective method for the optical manufacturing of silicon for its achievable high form accuracy, low subsurface damage and high surface integrity.

While Si is known as a typical brittle material, the ductile mode cutting is critical for achieving high machinability of the material. Two types of strategies are considered for the ductile mode cutting of Si. One is revealing the brittle-to-ductile (BTD) transition of Si in taper cutting trials, which derives the critical depth of cut (DOC) that will be used as a critical cutting parameter in

following turning processes [1–5]. The other is the modification of Si surface by various pre-treating methods, such as ion implanting, which increase the ductile machinability of Si [6–10]. In spite of above strategies, the machinability of Si also greatly depends on the extrinsic cutting parameters, in addition to intrinsic parameter such as crystallography orientation [11–15].

Therefore, in the present work we perform face turning experiments of Si using diamond tools. The influence of cutting parameters, such as rake angle of cutting tool, DOC and spindle speed, on cutting results in terms of machined surface topography and surface roughness is studied.

2. Experimental setup

Diamond cutting experiments are performed in the home-made ultra-precision CNC diamond turning lathe, as shown in Figure 1a. The lathe is jointly developed by Center for Precision Engineering, Harbin Institute of Technology and Research Center of Laser Fusion, China Academy of Engineering Physics. Table 1 lists the exact specifications of the lathe.

(a) (b)

Figure 1. Configuration of diamond turning of monocrystalline Si. (a) Experimental setup; (b) clamping apparatus.

The utilized specimen of monocrystalline Si has a crystallographic orientation of (010). The specimen has a dimension of 5 mm in length, 5 mm in width and 0.5 mm in thickness. Table 2 lists the specific parameters of the specimen. As illustrated in Figure 1b, four decentered pieces of Si specimen are placed on the aluminum alloy substrate with a thickness of 15 mm and a radius of 100 mm.

Single crystalline diamond cutting tools are used in the ultra-precision turning experiments. The cutting tool has a clearance angle of 7 °, a cutting edge radius of 100 nm and a nose radius of 0.2 mm. To investigate the influence of rake angle, four rake angles as 0 °, −15 °, −30 °and −45 °are considered. Table 3 lists the cutting parameters utilized in the face turning experiments, which shows that four spindle speeds and five DOCs are considered. After the turning experiments, the machined surface is characterized by scanning electron microscope (SEM) and white light interferometer, which respectively provides machined surface topography and surface roughness. The diameter of measuring area by the white light interferometer is 100 μm.

Table 1. Specifications of home-made ultra-precision diamond turning lathe.

Parameter	Value
Maximum spindle speed (rpm)	5000
Rotation accuracy (μm)	0.05
Slide stroke (mm)	X/Z: 200/200
Straightness (μm)	0.2 μm@full stroke
Positioning accuracy (μm)	1
Repositioning accuracy (μm)	0.2
Minimum Increment Amount of X- and Z-axis (nm)	10
Form accuracy	PV-0.15
Roughness	Rq-10

Table 2. Specifications of Si specimen.

Parameter	Value
Crystal orientation	(100)
Doping	P-doped
Resistivity (Ω·cm)	0.5~2
Dimension (mm)	5, 5 and 0.5

Table 3. Configurations of cutting parameters.

Parameter	Value
Tool rake angle	0 °, −15 °, −30 °, −45 °
Spindle speed (rpm)	1000, 2000, 3000, 4000
Depth of cut (μm)	0.1, 0.2, 0.3, 0.5, 1.0

3. Results and discussion

3.1. Effect of rake angle

The effect of rake angle of cutting tool on the cutting results of Si(100) is firstly carried out. Four rake angles, as 0 °, −15 °, −30 ° and −45 °, respectively, are employed. For each rake angle, the other cutting parameters are the same: the DOC is 0.2 μm, the spindle speed is 4000 rpm and the feed rate is 1.5 μm/r.

Figure 2 presents SEM images of Si(100) surface after diamond turning using different rake angles, which show that an ultra-smooth surface is obtained for the rake angle of 0 °. It should be noted that the SEM image with a higher magnification is hindered by the focusing difficulty due to extreme super finish surface. Specifically, only sporadic defects caused by material crushing are formed on the machined surface for the rake angle of 0 °. However, the defects become more pronounced for lower value of rake angle, which leads to deterioration of machined surface integrity. In particular for the rake angle of −45 °, there are considerable residual chip burrs formed on the machined surface due to uncompleted material removal, indicating a dominant brittle mode cutting.

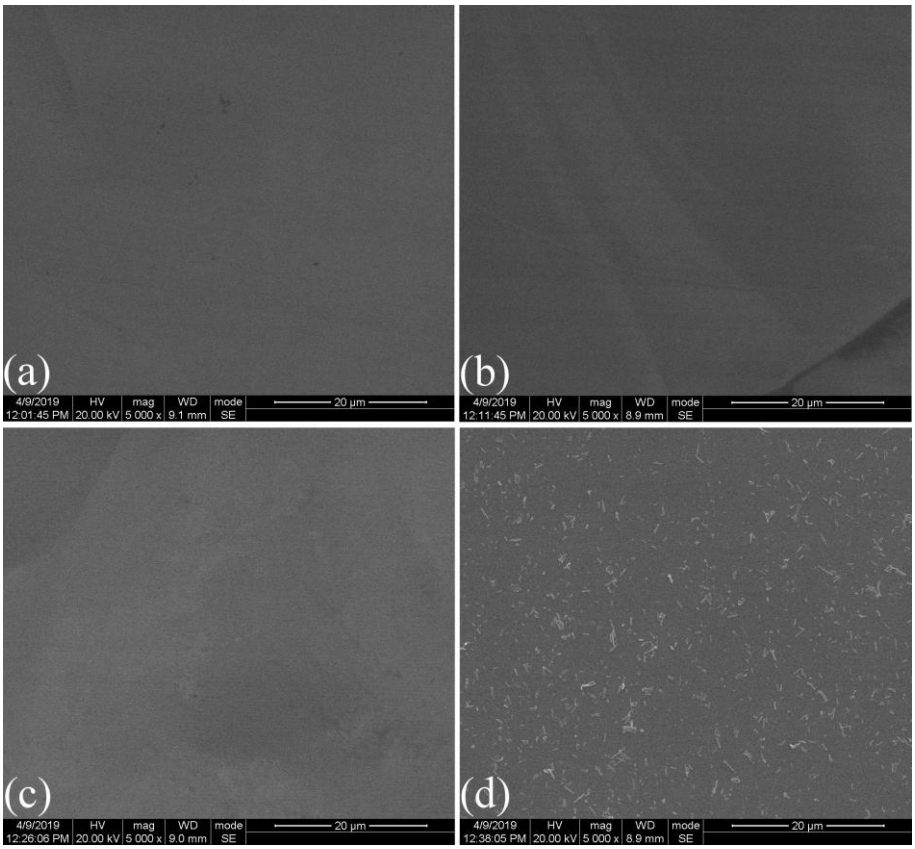

Figure 2. SEM images of machined surface after diamond turning using different rake angles. Rake angle: (a) 0 °; (b) −15 °; (c) −30 °; (d) −45 °.

Accordingly, Figure 3 presents images of Si(100) characterized by white light interferometer, which show that there are residual tool marks observed on machined surface for each rake angle. However, the residual tool marks become more pronounced for a lower rake angle. Specifically, Figure 3 shows that the medium and high frequency components in residual tool marks increase with decreasing rake angle, which leads to deterioration of surface flatness accompanied with the presence of cracks.

Figure 4 plots variations of surface roughness with utilized rake angle. For each rake angle, two measurements are made, and error bars are also presented in Figure 4. The surface roughness is the lowest as 5.9 nm for the largest rake angle of 0 °. With a decrease of rake angle, Figure 4 shows that the surface roughness first increases to 9.5 nm at a rake angle of −15 °, and then decreases to 8.0 nm at a rake angle of −30 °. With a further decrease of rake angle to −45 °, the surface roughness greatly increases to 18 nm. Therefore, it is suggested that the machined surface quality deteriorates with decreasing rake angle of cutting tool. The best machined surface quality can be achieved with a rake angle of 0 °. The utilization of a negative rake angle less than −30 ° facilitates the formation of local compressive hydrostatic pressure at the cutting zone, accompanied with the increase of shear plane length. However, the further decrease of rake angle into −45 ° leads to decrease of shear plane length and decrease of local compressive hydrostatic pressure at the cutting zone [16].

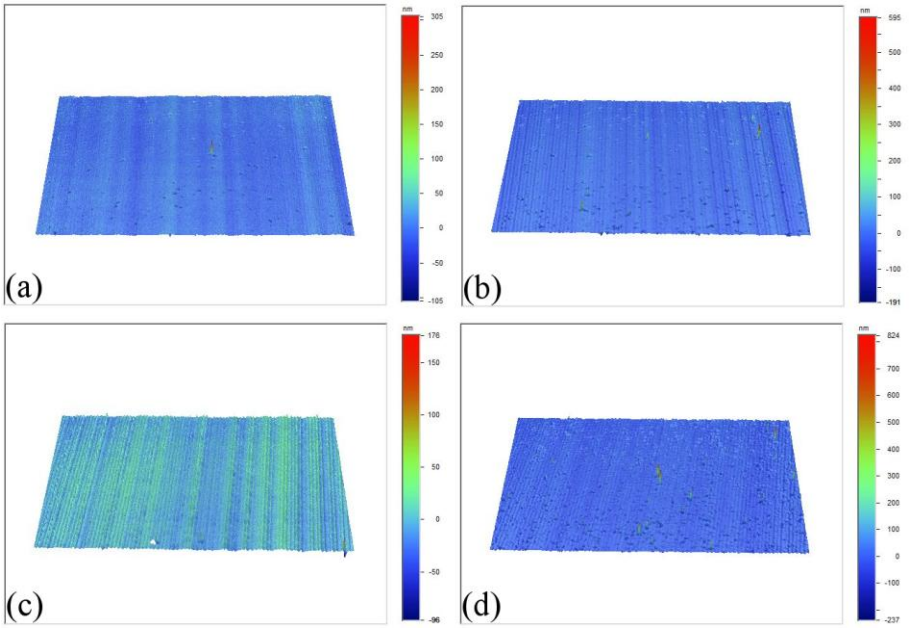

Figure 3. Topographies of machined surface characterized by white light interferometer. Rake angle: (a) 0 °; (b) −15 °; (c) −30 °; (d) −45 °.

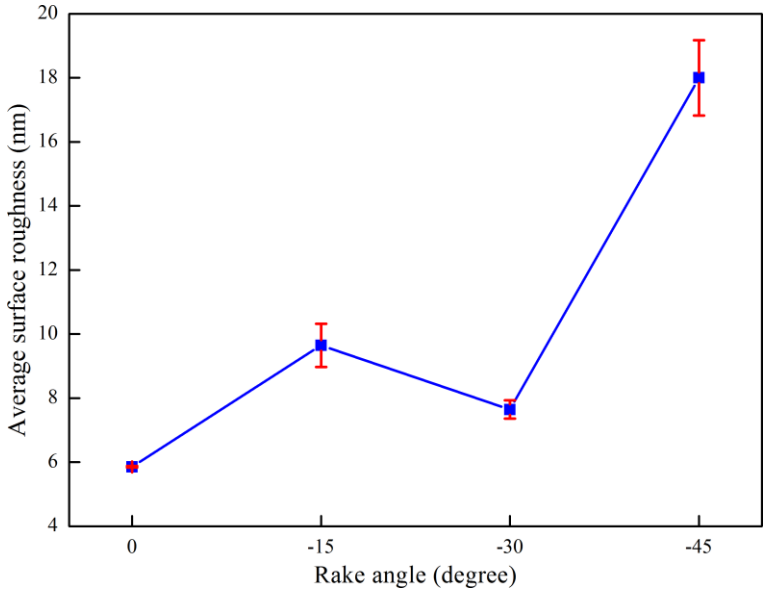

Figure 4. Achieved surface roughness of machined Si(100) surface for different rake angles.

3.2. Effect of DOC

The effect of DOC on the cutting results of Si is carried out. Five DOCs, as 0.1, 0.2, 0.3, 0.5 and 1.0 μm, are considered. For each DOC, the other cutting parameters are the same: the rake angle is 0 °, the spindle speed is 4000 rpm and the feed rate is 1.5 μm/r.

Figure 5 presents SEM images of Si surface after diamond turning using different DOCs, which shows that the DOC has a strong influence on the machined surface topography. As compared to the

Figure 2a with a DOC of 0.2 μm, the machined surface quality is lower for the other four DOCs. For the DOC of 0.1 μm, local trivial cracks are observed on machined surface. However, there are considerable residual chip burrs formed at the DOC of 0.3 μm. While the DOC increases to 0.5 μm, the local defect zones grow up to form areas with non-uniform shape. Figure 5d shows that the local defects disappear at the DOC of 1 μm, however, there are pronounced cracks formed on machined surface.

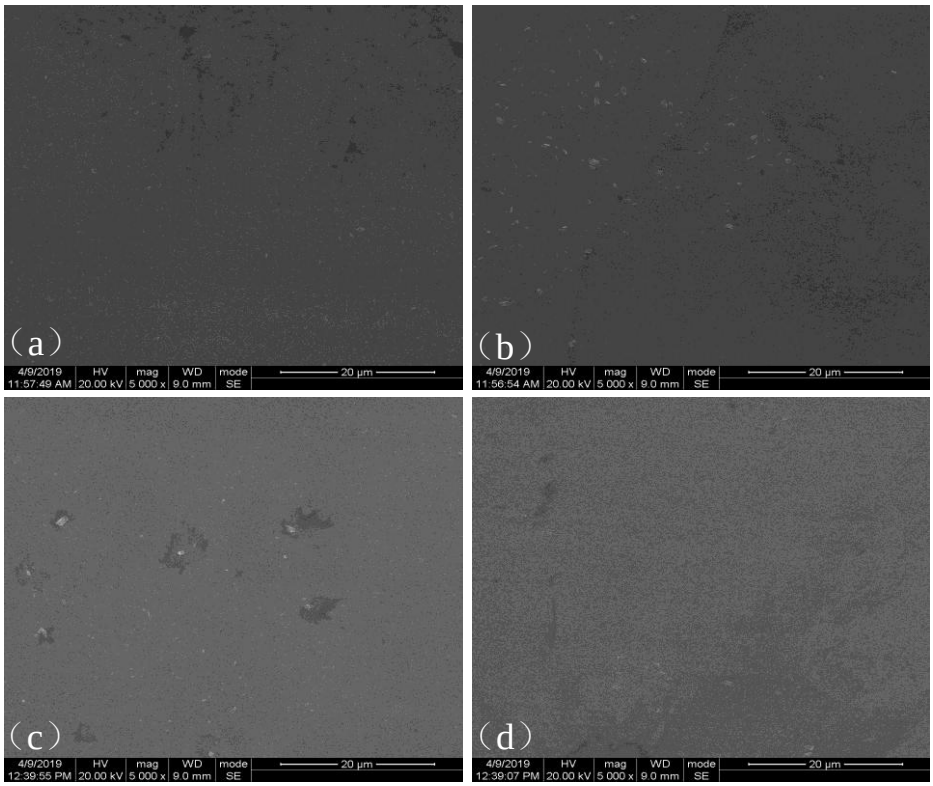

Figure 5. SEM images of machined surface after diamond turning using different DOCs. DOCs: (a) 0.1 μm; (b) 0.3 μm; (c) 0.5 μm; (d) 1.0 μm.

Accordingly, Figure 6 presents images of Si(100) surface characterized by white light interferometer, which show that there are considerable cracks observed on machined surface for each DOC. Figure 6 shows that the residual tool mark is not dependent on the DOC. However, the presence of surface cracks is more pronounced for a larger DOC. Figure 6 shows that with the increase of DOC, the surface integrity greatly deteriorates accompanied with the presence of cracks.

Figure 7 plots variations of surface roughness with utilized DOCs. For each DOC, two measurements are made, and error bars are also presented in Figure 7. Figure 7 demonstrates that with the increase of DOC from 0.1 to 0.2 μm, surface roughness decreases from 10.0 nm to 5.9 nm. With a further increase of DOC, however, surface roughness increases with increasing DOC, and reaches 15.0 nm at the DOC of 0.5 μm. The surface roughness for the DOC of 1 μm is lower than that for the 0.5 μm. Therefore, it is suggested that the best machined surface quality can be achieved with a low DOC of 0.2 μm.

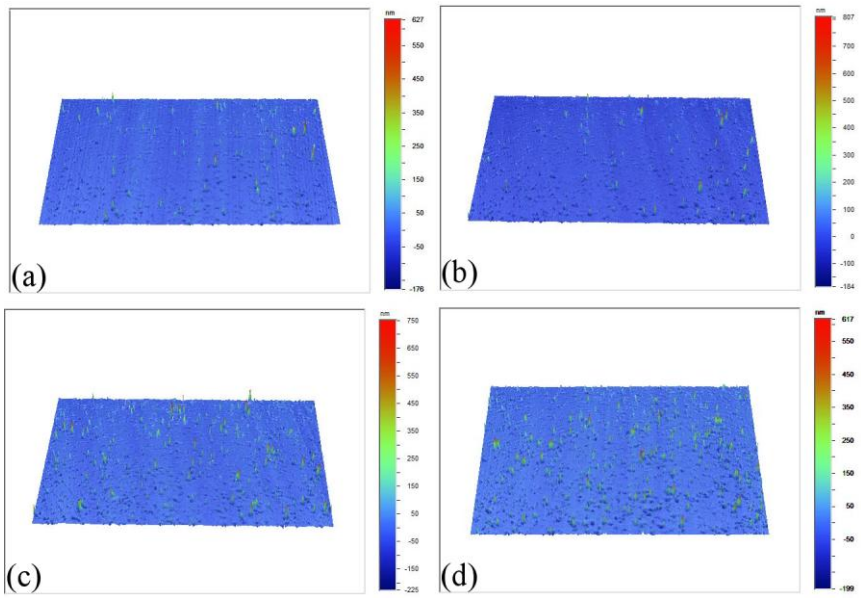

Figure 6. Topographies of machined surface characterized by white light interferometer. DOCs: (a) 0.1; (b) 0.3; (c) 0.5; (d) 1.0 μm.

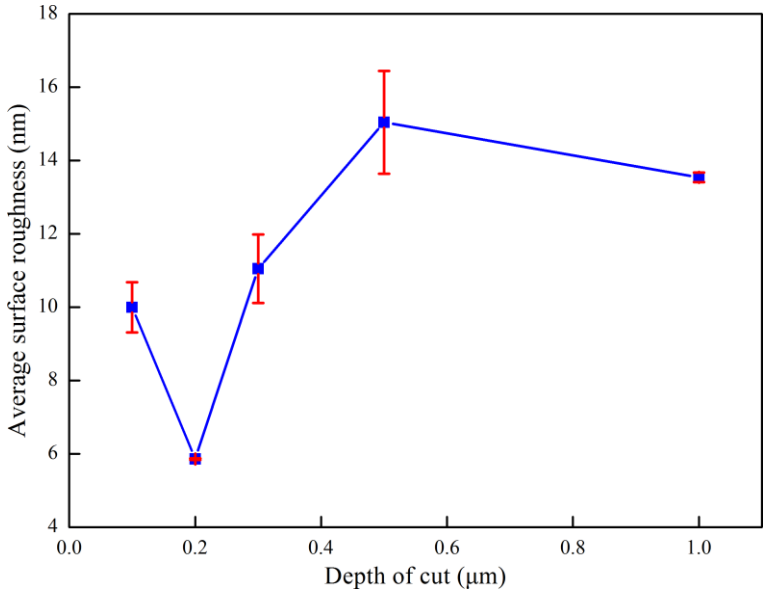

Figure 7. Achieved surface roughness of machined Si(100) surface for different DOCs.

3.3. Effect of spindle speed

To address the influence of cutting speed, cutting experiments with different spindle speeds are carried out. Four spindle speeds, as 1000, 2000, 3000 and 4000 rpm, are employed. For each spindle speed, the other cutting parameters are the same: the rake angle is 0 °, the DOC is 0.2 μm and the feed rate is 1.5 μm/r.

Figure 8 presents SEM images of Si surface after diamond turning using different spindle speeds, which shows that the spindle speed has a strongly influence on the machined surface

topography. Figure 8 shows that the machined surface integrity is the best for a spindle speed of 2000 rpm than the other three spindle speeds, as there are less pronounced residual tool marks and surface cracks formed. For the spindle speed of 1000 rpm, there are considerable cracks appeared on machined surface, which consequently deteriorates the surface integrity. With the further increase of spindle speed, there are more pronounced irregularly distributed local defects or cracks formed on machined surface.

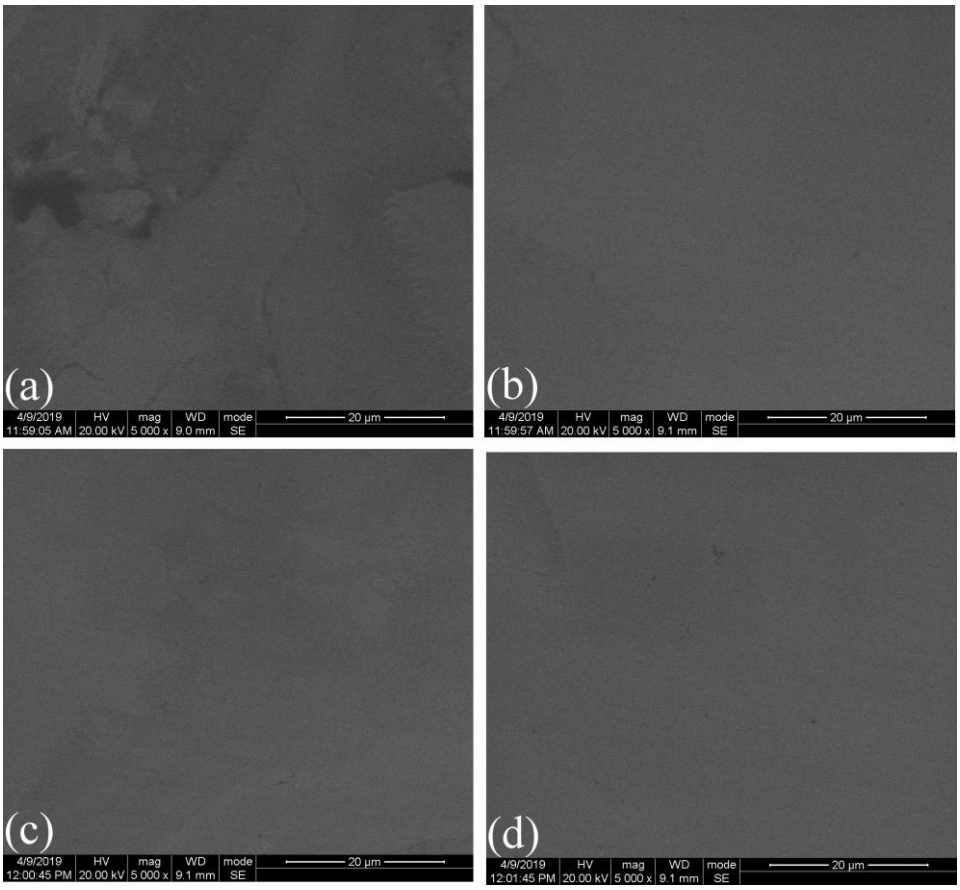

Figure 8. SEM images of machined surface after diamond turning using different spindle speeds. Spindle speed: (a) 1000; (b) 2000; (c) 3000; (d) 4000 rpm.

Accordingly, Figure 9 presents images of Si(100) surface characterized by white light interferometer, which shows that the machined surface has a high surface integrity with the absence of surface cracks for each spindle speed. Furthermore, there are residual tool marks observed on machined surface for each spindle speed. However, the residual tool marks are the least and the most pronounced for the spindle speed of 2000 rpm and 4000 rpm, respectively. For the spindle speed of 1000 rpm, the residual tool marks are obvious and uniform, the local defects caused by the material crushing are also identified. For the spindle speed of 2000 rpm, the residual tool marks are hard to distinguish. For the spindle speed of 3000 rpm, the residual tool marks grow up, and the distribution evenness reduces gradually. There are irregular grooves appeared on the machined surface, which reduce the surface integrity. For the spindle speed of 4000 rpm, the residual tool marks grow up and the distribution evenness reduces further.

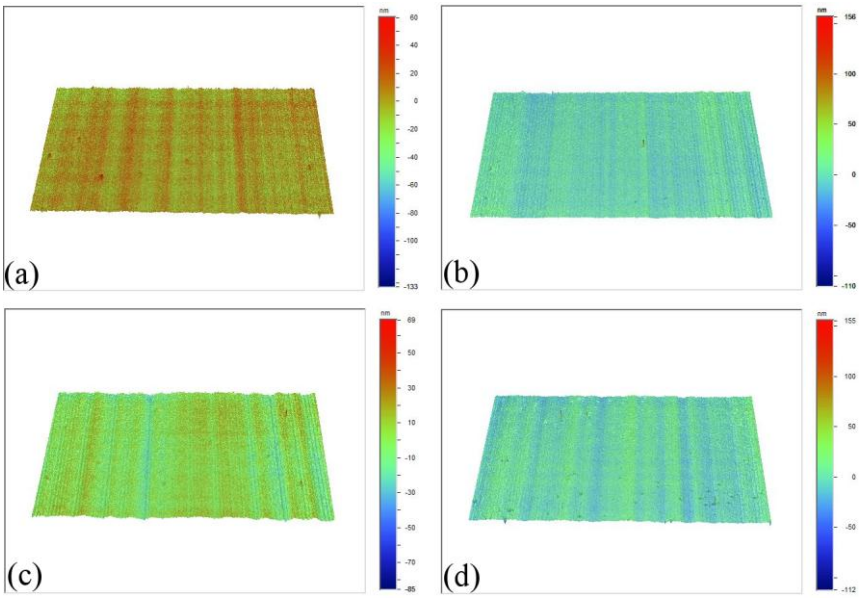

Figure 9. Topographies of machined surface characterized by white light interferometer. Spindle speed: (a) 1000; (b) 2000; (c) 3000; (d) 4000 rpm.

Figure 10 plots variations of surface roughness with utilized spindle speeds. For each spindle speed, two measurements are made, and error bars are also presented in Figure 10. Figure 10 demonstrates that with the increase of spindle speed from 1000 to 2000 rpm, surface roughness decreases from 4.8 nm to 4.5 nm, which is the minimum surface roughness achievable. With a further increase of spindle speed, however, surface roughness increases with increasing spindle speed, and reaches the maximum value of 5.9 nm at a spindle speed of 4000 rpm. Therefore, it is suggested that the best machined surface quality can be achieved with a spindle speed of 2000 rpm.

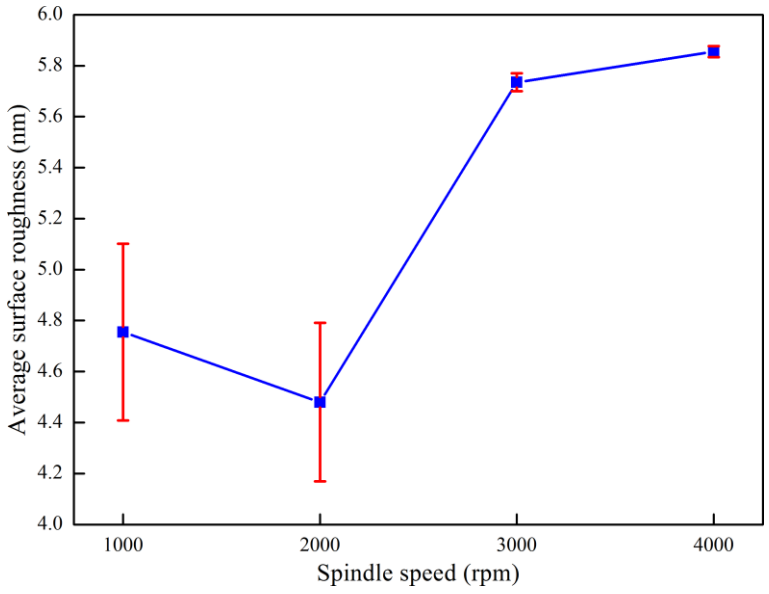

Figure 10. Achieved surface roughness of machined Si(100) surface for different spindle speeds.

4. Conclusion

In summary, we perform ultra-precision diamond turning experiments of monocrystalline silicon (100) to achieve an ultra-smooth machined surface, with an emphasis on the influence of cutting parameters on machining results. Experimental results show that the topography and surface integrity of machined surface can be greatly affected by the rake angle of cutting tool, the DOC and the spindle speed. Specifically, an optimized combination of cutting parameters (a rake angle of 0 °, a DOC of 0.2 μm and a spindle speed of 2000 rpm) is discovered, which leads to the best machined surface quality of Si(100) with a lowest surface roughness of 4.5 nm.

Acknowledgement

This work was supported by the Foundation of Laboratory of Ultra Precision Manufacturing Technology, CAEP (ZD 18007), the Science Challenge Project (No. TZ2018006-0201-02 and TZ2018006-0205-02).

Conflict of interest

The authors declare that they have no conflict of interest.

Reference

1. Goel S, Luo X, Comley P, et al. (2013) Brittle–ductile transition during diamond turning of single crystal silicon carbide. *Int J Mach Tool Manu* 65: 15–21.
2. Zhou M, Ngoi BKA, Zhong ZW, et al. (2001) Brittle-ductile transition in diamond cutting of silicon single crystals. *Mater Manuf Process* 16: 447–460.
3. Xiao G, To S, Zhang G (2015) Molecular dynamics modelling of brittle–ductile cutting mode transition: case study on silicon carbide. *Int J Mach Tool Manu* 88: 214–222.
4. Wang MH, Lu ZS (2008) Study on brittle-ductile transition mechanism of ultra-precision turning of single crystal silicon. *Key Eng Mater* 375: 11–16.
5. Mukaiyama K, Ozaki M, Wada T (2017) Study on ductile-brittle transition of single crystal silicon by a scratching test using a single diamond tool. *2017 8th International Conference on Mechanical and Aerospace Engineering (ICMAE)*, 40–44.
6. Xiao GB, To S, Jelenković EV (2015) Effects of non-amorphizing hydrogen ion implantation on anisotropy in micro cutting of silicon. *J Mater Process Tech* 225: 439–450.
7. To S, Wang H, Jelenković EV (2013) Enhancement of the machinability of silicon by hydrogen ion implantation for ultra-precision micro-cutting. *Int J Mach Tool Manu* 74: 50–55.
8. Wang JS, Zhang XD, Fang FZ, et al. (2019) Diamond cutting of micro-structure array on brittle material assisted by multi-ion implantation. *Int J Mach Tool Manu* 137: 58–66.
9. Wang JS, Zhang XD, Fang FZ (2016) Molecular dynamics study on nanometric cutting of ion implanted silicon. *Comp Mater Sci* 117: 240–250.
10. Fang FZ, Chen YH, Zhang XD, et al. (2011) Nanometric cutting of single crystal silicon surfaces modified by ion implantation. *CIRP Ann* 60: 527–530.

11. Wang M, Wang W, Lu Z (2012) Anisotropy of machined surfaces involved in the ultra-precision turning of single-crystal silicon—a simulation and experimental study. *Int J Adv Manuf Tech* 60: 473–485.
12. Cheung CF, To S, Lee WB (2002) Anisotropy of surface roughness in diamond turning of brittle single crystals. *Mater Manuf Process* 17: 251–267.
13. Kobaru Y, Kondo E, Iwamoto R (2012) Ultra-precision cutting of single crystal silicon using diamond tool with large top corner radius. *Key Eng Mater* 523: 81–86.
14. Kobaru Y, Kondo E, Iwamoto R (2017) Precision cutting of single crystal silicon using CBN tool with large top corner radius. *Int J Nanomanuf* 13: 170–184.
15. Abdulkadir LN, Abou-El-Hossein K, Jumare AI, et al. (2018) Ultra-precision diamond turning of optical silicon—a review. *Int J Adv Manuf Tech* 96: 173–208.
16. Zhang JJ, Han L, Zhang JG, et al. (2019) Finite element analysis of the effect of tool rake angle on brittle-to-ductile transition in diamond cutting of silicon. *Int J Adv Manuf Tech*. Available from: https://doi.org/10.1007/s00170-019-03888-8.

AIMS Press